Biophysical Methods

Deutsche Ausgabe: DOI: 10.1002/ange.201605284
Internationale Ausgabe: DOI: 10.1002/anie.201605284

Direct Identification of Protein–Protein Interactions by Single-Molecule Force Spectroscopy

Andrés M. Vera and Mariano Carrión-Vázquez**

Abstract: *Single-molecule force spectroscopy based on atomic force microscopy (AFM-SMFS) has allowed the measurement of the intermolecular forces involved in protein-protein interactions at the molecular level. While intramolecular interactions are routinely identified directly by the use of polyprotein fingerprinting, there is a lack of a general method to directly identify single-molecule intermolecular unbinding events. Here, we have developed an internally controlled strategy to measure protein–protein interactions by AFM-SMFS that allows the direct identification of dissociation force peaks while ensuring single-molecule conditions. Single-molecule identification is assured by polyprotein fingerprinting while the intermolecular interaction is reported by a characteristic increase in contour length released after bond rupture. The latter is due to the exposure to force of a third protein that covalently connects the interacting pair. We demonstrate this strategy with a cohesin–dockerin interaction.*

Atomic force microscopy based single-molecule force spectroscopy (AFM-SMFS) has allowed quantification of the mechanical strength of protein–protein interactions, estimation of their kinetic constants, and exploration of the corresponding energy landscapes.[1,2] In the classical experimental configuration, the force and extension of a pair of interacting proteins are measured. Typically, polymeric linkers are used to attach the proteins of the pair, one to the AFM tip and the other to a substrate.[1,3] However, in this experimental set up, it is challenging to assure single-molecule conditions and to differentiate the rupture event from unspecific tip–surface adhesion or breakage of the protein attachments.[4,5] As a result, it is impossible to directly identify the event of bond breakage in the recordings.[6]

Recent alternative strategies are based on the inclusion of polyproteins in the interacting partners. This approach exploits the recognizable pattern of polyproteins to assure single-molecule conditions.[7–11] However, these strategies either cannot discriminate unbinding events originating from desorption of protein from the tip/substrate surfaces[10] or they rely on well-known specific topological and unfolding features of the interacting proteins in order to identify the rupture events.[7–9,11] Altogether, these drawbacks limit the usefulness of these strategies since they are case dependent and not generally applicable.

Herein, we propose a general internally-controlled design that allows direct identification of the rupture event in the AFM-SMFS recordings while maintaining single-molecule conditions. Our strategy is based on the fusion of a single-molecule marker (a small polyprotein formed by 3 repeats of the I27 module)[12] to each interacting protein, and on the addition of a second marker, in parallel to the interacting pair, which is a force-compliant polypeptide covalently bound by disulfide-bonded cysteines (Figure 1 A).This polypeptide is mechanically protected by the interaction so that breakage of the interaction is needed in order to expose it to force (Figure 1 B). As a result, the force peak originating from the rupture of the intermolecular interaction is followed by a ΔL_c value related to the polypeptide L_c[13] (contour length, the end-to-end distance of the polymer).

We implemented this strategy in the high-affinity cohesin–dockerin interaction from the cellulosome of *Clostridium thermocellum*,[14] applying tension from the C-terminus of the proteins.

Since the interacting pair and the connecting polypeptide are stretched in parallel, in order to be force-hidden, this polypeptide has to be very compliant to force during the first stages of extension, so that the mechanical load is mainly transmitted through the interaction. A random-coil protein with a larger L_c than the length of the interacting complex fulfills this requirement, and for this reason we used 12 resilin-derivative repeats[15] (12xR, $L_c \approx 83$ nm, referred to hereafter as the "elastomer") as the connecting polypeptide.

Formation of the desired disulfide bonds between engineered cysteines of the three recombinant constructs is governed by "Velcro" oligomerization domains[16] that bring the cysteines of the partner proteins together in favorable orientations. To implement the selected configuration for stretching (C–C terminal), three different domains were designed: two acidic (Acid1 and Acid2), and one basic (Basic). The acidic domains were set on both sides of the elastomer, near the N- and C-termini, while the proteins carrying cohesin and dockerin have the same basic domain. The acidic domains interact heteromerically with the basic domain, forming antiparallel or parallel heterodimers for Acid1 or Acid2, respectively (Figure 1 A and Figure S1A,B in the Supporting Information).

We tested the ability of the oligomerization domains to drive disulfide bond formation. To this end, we co-incubated

[*] Dr. A. M. Vera, Dr. M. Carrión-Vázquez
Instituto Cajal, Consejo Superior de Investigaciones Científicas
Avda. Doctor Arce 37, E-28002 Madrid (Spain)
E-mail: mcarrion@cajal.csic.es
avera@cajal.csic.es
Homepage: http://www.cajal.csic.es/ingles/departamentos/carrion-vazquez/carrion-vazquez.html
http://carrionvazquez-lab.org/en/index.cfm
Dr. A. M. Vera, Dr. M. Carrión-Vázquez
Instituto Madrileño de Estudios Avanzados en Nanociencia (IMDEA-Nanociencia), E-28049 Cantoblanco, Madrid (Spain)

Supporting information for this article can be found under: http://dx.doi.org/10.1002/anie.201605284.

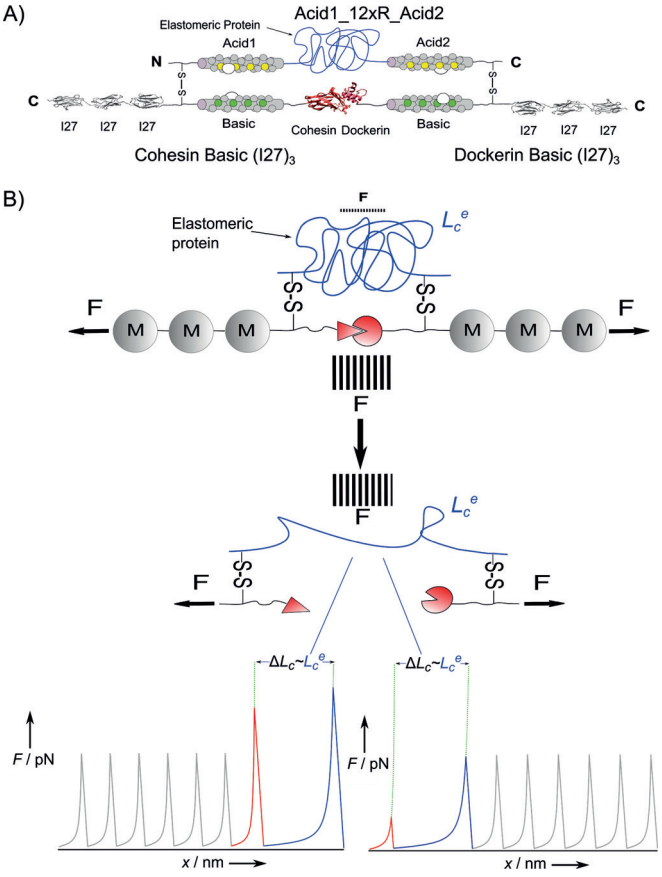

Figure 1. A schematic of our "parallel staple" strategy to study protein–protein interactions by AFM-SMFS. A) An illustration of the final constructs, showing all the key components. B) The sawtooth pattern generated by the unfolding of the marker modules (gray) ensures single-molecule identification. The rupture of the interaction (red) is reported by the ΔL_c generated from a force-hidden elastomeric protein (blue) connected in parallel in the mechanical circuit.

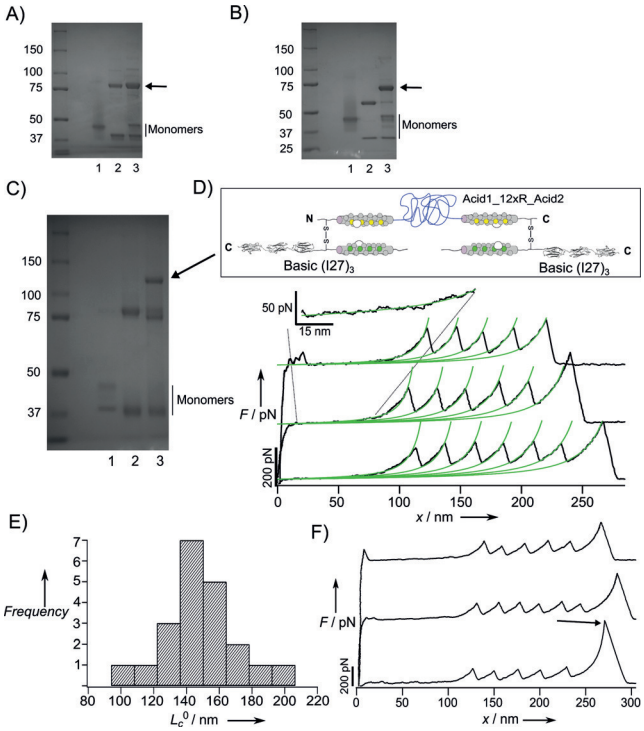

Figure 2. Characterization of the key components of the system. A–C) Non-reducing SDS-PAGE. The presence of bands with MW higher than the monomers indicates the ability of the oligomerization domains to drive disulfide bond formation. A) Lane 1: Acid1(I27)$_3$, lane 2: Basic(I27)$_3$, lane 3: both. The arrow indicates Acid1(I27)$_3$/Basic(I27)$_3$ heterodimers. B) Lane 1: Acid1(I27)$_3$, lane 2:Basic(GB1)$_3$, lane 3: both. The arrow indicates Acid1(I27)$_3$/Basic(GB1)$_3$ dimers. C) Lane 1: Acid1_12xR_Acid2, Lane 2: Basic(I27)$_3$, lane 3: both. The arrow indicates one molecule of Acid1_12xR_Acid2 bound to two molecules of Basic(I27)$_3$. D) The empty control construct (top) and several AFM-SMFS recordings from this construct. Green solid lines are WLC fits. E) L_C^0 histogram from recordings of the empty construct carrying six I27 markers. F) Recordings showing high detachment forces (last force peak).

short polyproteins carrying complementary Velcro peptides (Basic(I27)$_3$/Acid1(I27)$_3$, and Basic(GB1)$_3$/Acid1(I27)$_3$, Figure S1C,D) in an oxidant redox buffer, and analyzed the reaction by non-reducing sodium dodecyl sulfate polyacrylamide gel electrophoresis (SDS-PAGE). The co-incubation of Basic(I27)$_3$ and Acid1(I27)$_3$ samples led to the appearance in SDS-PAGE of a band of higher intensity and slightly higher molecular weight (MW) than the Basic(I27)$_3$ homodimer (arrow in lane 3 vs. lane 2, respectively; Figure 2A, and Figure S2A). Although this result confirms the formation of disulfide bonds, the similar electrophoretic mobility of the Basic(I27)$_3$ homodimer and the Basic(I27)$_3$/Acid1(I27)$_3$ heterodimer makes it difficult to assess the preferential formation of heterodimers. In the case of Basic(GB1)$_3$/Acid1(I27)$_3$ samples, thanks to the smaller size of the GB1 module,[17] we can clearly confirm the preferential heterodimeric formation in the desired orientation by electrophoresis (Lane 3, Figure 2B, and Figure S2B). Disulfide bond formation between polyproteins was corroborated by AFM-SMFS experiments showing the typical patterns of homo- and heteropolyproteins (Figure S2C,D).

A simplified experimental strategy was designed in order to test the behavior of each of the components; namely the elastomer, single-molecule markers, and oligomerization domains. Here, the Cohesin/Dockerin Basic(I27)$_3$ constructs were substituted with Basic(I27)$_3$ carrying a mock sequence (GGSG) instead of the cohesin/dockerin pair (cartoon, Figure 2D). This empty construct also serves as a negative control since it is not expected to produce any force peak.

Figure 2C shows a non-reducing SDS-PAGE of Basic(I27)$_3$ + Acid1_12xR_Acid2 samples after incubation in an oxidant redox buffer. Co-incubation of the two proteins yields the formation of three bands with higher MW than the monomers. The comparison of these samples with the isolated Basic(I27)$_3$ sample allows us to identify the middle band as Basic(I27)$_3$ homodimers. Based on their MW, the lower and the upper bands can be assigned to one molecule of Acid1_12xR_Acid2 bound to either one molecule of Basic(I27)$_3$ or two molecules of Basic(I27)$_3$, respectively (lane 3, Figure 2C). Titration experiments support this interpretation and also indicate that the population of Acid1_12xR_Acid2

bound to two molecules of Basic $(I27)_3$ can be maximized (Figure S3A).

The stretching from the C-termini of the Basic$(I27)_3$ molecules by AFM-SMFS should show two types of events in the recordings: the extension of the elastomer from Acid1_12xR_Acid2 and the unfolding of 4–6 I27 modules. In the recordings ($n = 56$), we clearly identify both markers (Figure 2D) since the traces show an initial region devoid of force peaks, which corresponds to the 12xR marker, followed by a sawtooth-pattern region of 4–6 peaks, which corresponds to the I27 markers ($\langle \Delta L_c \rangle = 28 \pm 0.9$ nm). The long initial region behaves as an entropic spring, fitting to the WLC model of polymer elasticity[13] without force peaks (Figure 2D, expanded section), resembling the features of a random coil, as expected for the 12xR repeats.[15] The random-coil features of the 12xR construct were further confirmed by circular dichroism measurements (Figure S3B).

These recordings only show the unfolding of the I27 modules and the entropic behavior of the 12xR repeats. This indicates that either the oligomerization domains unfold with no detectable mechanostability, or that they do so with such a high mechanical stability that the mechanical circuit always breaks before their unfolding. Since a similar leucine zipper in the same configuration was reported to have no detectable mechanostability upon stretching,[18] and considering the high detachment forces displayed in some recordings (up to 630 pN, arrow Figure 2F), the most likely scenario is the first one. Assuming that the Velcro peptides do not show detectable mechanostability, the L_C^0 (L_c of the first force peak) of the molecule can be estimated as (ca. 5 nm) × 6 folded I27 + 0.4 nm/residues[19] × 280 residues (domains + 12xR) = 142 nm. Figure 2E shows the L_C^0 histogram of molecules with six I27 repeats ($n = 25$), with $\langle L_C^0 \rangle = 147 \pm 24$ nm, which is in good agreement with the calculated value. This supports the idea that the oligomerization domains unfold with no detectable mechanical resistance.

Finally, we performed nanomechanical characterization of the cohesin/dockerin constructs. First, the Cohesin/Dockerin Basic$(I27)_3$ complex was co-incubated with Acid1_12xR_Acid2 in the proper redox buffer, and the formation of disulfide bonds was confirmed (Figure 3A). In the AFM-SMFS experiments, only recordings displaying 4–6 I27 force peaks were selected for analysis. This criterion ensures both single-molecule conditions and that the cohesin–dockerin interaction has been subjected to force. As in the case of the empty construct (blue trace, Figure 3B), the cohesin/dockerin recordings show the typical fingerprint of 4–6 I27 modules ($\langle \Delta L_c \rangle = 27.9 \pm 0.7$ nm); however, these curves show an additional force peak that is weaker than those of I27 (red traces, Figure 3B). The ΔL_c of the former shows low variability (Figure 3C,D). Strong evidence that this force peak originates from the rupture of a cohesin–dockerin interaction is given by the presence of the two markers included in the experimental design: 1) 4–6 I27 repeats; 2) the existence of a force peak with a discrete ΔL_c (absent in the empty control).

The ΔL_c histogram of the cohesin–dockerin force peak shows a maximum around 70 nm; $\langle \Delta L_c \rangle = 70 \pm 6$ nm (Figure 3D). The expected value can be approximated as the difference between the L_c when the cohesin and dockerin are

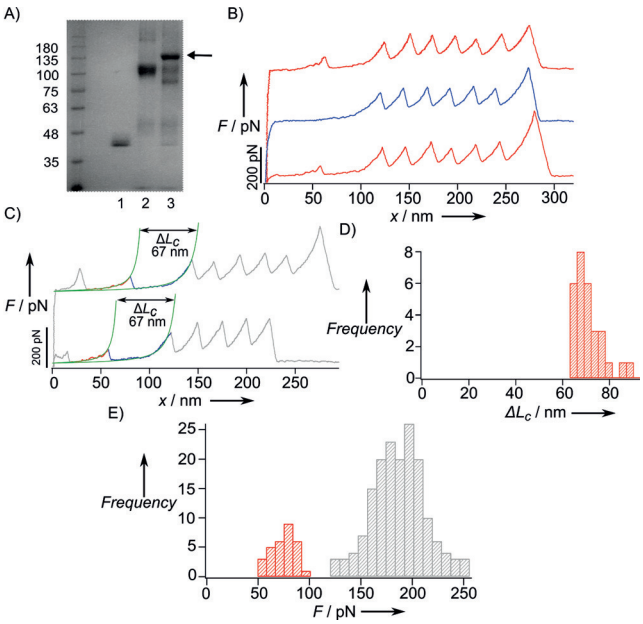

Figure 3. Mechanostability of the cohesion–dockerin interaction. A) SDS-PAGE. Lane 1: Acid1_12xR_Acid2; lane 2: Cohesin/Dockerin Basic$(I27)_3$, lane 3: both. The arrow indicates the Cohesin/Dockerin Basic$(I27)_3$ complex disulfide-bonded to the elastomer. B) Comparison of recordings from cohesin/dockerin (red) and the empty control (blue). C) WLC fits (green) of two cohesin/dockerin recordings. D) ΔL_C histogram of the cohesin–dockerin rupture force peak. E) Force histogram. I27 unfolding events are shown in gray, cohesin–dockerin unbinding events in red ($n = 30$ recordings).

interacting (L_c^I) and the L_c once the interaction has been dissociated ($L_c^D = L_c^0$ of the empty model, 142 nm). L_c^I = 5 nm × (6 I27) + 5 nm of the cohesin–dockerin complex[20] + 0.4 nm × 90 residues (domains) = 71 nm. The expected ΔL_c of 71 nm is in good agreement with the experimental value. Control experiments using a different elastomer with larger L_c generate larger ΔL_c values (Figure S5), thus confirming the robustness of our experimental design.

The force histogram (Figure 3E) displays two populations, one corresponding to the unfolding of the I27 marker ($\langle F \rangle = 187 \pm 26$ pN),[12] and another with a lower mechanostability (75 ± 12 pN) corresponding to cohesin–dockerin unbinding (F_D). This F_D value is in the range of what has been reported for a related cohesin/dockerin pair also from *C. thermocellum*.[21]

In conclusion, we have developed an internally controlled strategy for studying protein–protein interactions by AFM-SMFS that enables direct identification of the dissociation force peak while ensuring single-molecule control. The strategy is of general applicability, since it does not depend on the nature or the specific characteristics of the proteins of interest. Single-molecule control is provided by the fusion of polyprotein markers to the proteins of interest while the reporter for the interaction force peak consists of the release of a distinctive ΔL_c, which results from the exposure of an elastomer to force upon rupture of the interaction. These results provide a proof of concept that a general and self-controlled single-molecule strategy to measure protein–

protein interactions in protein nanomechanics is possible. This development paves the way towards a universal method to measure protein–protein interactions by AFM-SMFS.

Acknowledgements

We thank Dr. Douglas V. Laurents for critical reading of the manuscript. The authors wish to acknowledge financial support from the Seventh Framework Programme in Nanosciences, nanotechnologies, materials & new production technologies (7PM -NMP 2013-17, 604530-2), the Joint Programming in Neurodegenerative Diseases (JPND 2015-17, AC14/00037), the ERA-IB-ERANET-2013-16 (EIB.12.022), and the Spanish National Programme 2013-16 (SAF2013-49179-C2-1-R).

Keywords: atomic force microscopy · biophysical methods · polyproteins · protein–protein interactions · single-molecule force spectroscopy

How to cite: *Angew. Chem. Int. Ed.* **2016**, *55*, 13970–13973
Angew. Chem. **2016**, *128*, 14176–14179

[1] P. Hinterdorfer in *Nanotribology and Nanomechanics* (Ed.: B. Bhushan), Springer, Berlin, **2005**, pp. 283–312.
[2] C. K. Lee, Y. M. Wang, L. S. Huang, S. Lin, *Micron* **2007**, *38*, 446–461.
[3] A. Fuhrmann, R. Ros, *Nanomedicine* **2010**, *5*, 657–666.
[4] J. W. Weisel, H. Shuman, R. I. Litvinov, *Curr. Opin. Struct. Biol.* **2003**, *13*, 227–235.
[5] C. Zhu, M. Long, S. E. Chesla, P. Bongrand, *Ann. Biomed. Eng.* **2002**, *30*, 305–314.
[6] R. Merkel, *Phys. Rep.* **2001**, *346*, 343–385.
[7] M. Bertz, M. Wilmanns, M. Rief, *Proc. Natl. Acad. Sci. USA* **2009**, *106*, 13307–133310.
[8] M. Bertz, J. Chen, M. J. Feige, T. M. Franzmann, J. Buchner, M. Rief, *J. Mol. Biol.* **2010**, *400*, 1046–1056.
[9] F. Berkemeier, M. Bertz, S. Xiao, N. Pinotsis, M. Wilmanns, F. Gräter, M. Rief, *Proc. Natl. Acad. Sci. USA* **2011**, *108*, 14139–14144.
[10] M. Kim, C.-C. Wang, F. Benedetti, P. E. Marszalek, *Angew. Chem. Int. Ed.* **2012**, *51*, 1903–1906; *Angew. Chem.* **2012**, *124*, 1939–1942.
[11] M. Bertz, J. Buchner, M. Rief, *J. Am. Chem. Soc.* **2013**, *135*, 15085–15091.
[12] M. Carrion-Vazquez, A. F. Oberhauser, S. B. Fowler, P. E. Marszalek, S. E. Broedel, J. Clarke, J. M. Fernandez, *Proc. Natl. Acad. Sci. USA* **1999**, *96*, 3694–3699.
[13] C. Bustamante, J. F. Marko, E. D. Siggia, S. Smith, *Science* **1994**, *265*, 1599–1600.
[14] M. E. Himmel, Q. Xu, Y. Luo, S.-Y. Ding, R. Lamed, E. A. Bayer, *Biofuels* **2010**, *1*, 323–341.
[15] S. Lv, D. M. Dudek, Y. Cao, M. M. Balamurali, J. Gosline, H. Li, *Nature* **2010**, *465*, 69–73.
[16] M. G. Oakley, P. S. Kim, *Biochemistry* **1998**, *37*, 12603–12610.
[17] Y. Cao, C. Lam, M. Wang, H. Li, *Angew. Chem. Int. Ed.* **2006**, *45*, 642–645; *Angew. Chem.* **2006**, *118*, 658–661.
[18] A. Sarkar, S. Caamano, J. M. Fernandez, *Biophys. J.* **2007**, *92*, L36–38.
[19] S. R. Ainavarapu, J. Brujic, H. H. Huang, A. P. Wiita, H. Lu, L. Li, K. A. Walther, M. Carrion-Vazquez, H. Li, J. M. Fernandez, *Biophys. J.* **2007**, *92*, 225–233.
[20] A. L. Carvalho, F. M. Dias, J. A. Prates, T. Nagy, H. J. Gilbert, G. J. Davies, L. M. Ferreira, M. J. Romao, C. M. Fontes, *Proc. Natl. Acad. Sci. USA* **2003**, *100*, 13809–13814.
[21] S. W. Stahl, M. A. Nash, D. B. Fried, M. Slutzki, Y. Barak, E. A. Bayer, H. E. Gaub, *Proc. Natl. Acad. Sci. USA* **2012**, *109*, 20431–20436.

Received: May 30, 2016
Revised: July 7, 2016
Published online: October 13, 2016

